

## Effect of auxiliary substances on the adsorption of anionic dyes on low-moor peat

Agnieszka Dzieniszewska\*, Joanna Kyzioł-Komosińska, Magdalena Pająk

*Institute of Environmental Engineering, Polish Academy of Sciences, 34 M. Skłodowska-Curie Str., 41-819 Zabrze, Poland, Tel. +48 32 271 64 81; emails: agnieszka.dzieniszewska@ipis.zabrze.pl (A. Dzieniszewska), joanna.kyziol-komosinska@ipis.zabrze.pl (J. Kyzioł-Komosińska), magdalena.pajak@ipis.zabrze.pl (M. Pająk)*

Received 5 April 2019; Accepted 19 September 2019

---

### ABSTRACT

The effect of auxiliary substances (NaCl, Na<sub>2</sub>CO<sub>3</sub>, and CH<sub>3</sub>COOH) used in real dyeing processes on the adsorption capacity of low-moor peat for reactive dyes (Reactive Blue 19, Reactive Blue 81, Reactive Black 5) and acid dyes (Acid Black 1, Acid Blue 9) was investigated. The adsorption of the dyes was studied as a function of dye concentration (1–1,000 mg L<sup>-1</sup>) and the properties of peat, using a batch method. The experimental data were analyzed using the Langmuir, Freundlich, Dubinin–Radushkevich, and Sips isotherm models. The effect of auxiliary substances depended on the dye-adsorbent system – the lower the binding ability of the dye on the peat, the greater the effect of the substances. The maximum dyes adsorption capacity and the affinity of the binding sites increased in the presence of auxiliaries in the solution. The presence of CH<sub>3</sub>COOH was an important factor since H<sup>+</sup> in the solution affected the peat surface charge by protonation reaction and the possibility of binding anionic dyes via electrostatic interaction. Only CH<sub>3</sub>COOH at low pH affected the peat surface charge because of the very good buffering capacity of peat. NaCl and Na<sub>2</sub>CO<sub>3</sub> increased the intermolecular forces as well as the dimerization process of reactive dyes in the solution. The Sips equation fitted the experimental results best. This model combines the Langmuir and Freundlich equations, suggesting that the mechanism of dyes binding is more complex and does not follow an ideal monolayer adsorption.

*Keywords:* Adsorption; Anionic dyes; Peat; Adsorption isotherms; Auxiliary substances

---

### 1. Introduction

Various industries (textiles, leather, pulp and paper, food and plastics) discharge wastewater polluted with dyes and pigments into the environment, with the textile industry being the main producer of colored wastewater. It is estimated that the textile industry uses around 50% of the total dye production, that is,  $4.5 \times 10^5$  tons of dyes per year [1]. During the dyeing of fibers and fabrics, 2%–50% of the dye used goes to wastewater, due to the different degrees of fixation various dye classes on fibers, and the greatest loss in effluent occurs for reactive dyes [2].

Reactive and acid dyes are the most widely used dyes in the textile industry. Reactive dyes are mainly used for dyeing cotton, wool, silk and nylon [3] and acid dyes are used for dyeing natural and acrylic fibers and other materials, such as leather and paper [4].

Many dyes or their metabolites are carcinogenic, teratogenic or mutagenic to humans and other living organisms [5]. Moreover, the dyes that are present in effluents after discharge into natural waters can modify the aquatic systems as they give water undesirable color, affect the oxygen distribution and reduce sunlight penetration, causing problems in the functioning and development of aquatic flora

---

\* Corresponding author.

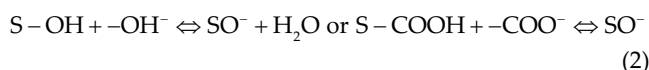
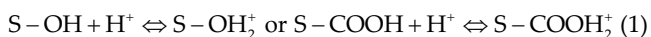
and fauna [6,7]. Therefore, there is no doubt that they should be removed from wastewater before disposal.

However, the treatment of colored wastewaters presents certain problems due to the chemical structure and properties of dyes. Dyes are resistant to biodegradation and photodegradation, as well as oxidizing agents [7–9]. Moreover, wastewater from the textile industry has a complex chemical composition. In addition to the significant amount of dyes, wastewater also contains auxiliary substances. Auxiliaries facilitate the binding of dyes to fibers and are present in wastewater in concentrations similar to that in which they were used [10]. Auxiliary substances include wetting agents, dispersants, dye fixing agents, and reducing and oxidizing agents. The quantity and type of auxiliaries depend on the type of fiber, the type of dye and the technology used for dyeing. Simple chemical compounds such as inorganic salts, bases, and acids as well as polymers and surfactants are used as auxiliary substances [11]. For example, NaCl is used to accelerate the diffusion and adsorption of dye molecules on fibers and to improve the fixation degree, Na<sub>2</sub>CO<sub>3</sub> as a pH-regulator in the dyeing of cellulose fibers with reactive dyes, and CH<sub>3</sub>COOH for pH adjustment in the dyeing of wool fibers with reactive and acid dyes [12,13]. The salts can affect the adsorption capacity of fibers by changing their surface charge and by changing the ionic nature, hydrophobicity and solubility of the dye [14].

One of the effective methods to remove dyes from aqueous solutions and wastewater is adsorption and biosorption by the use of organic materials, such as carbonaceous substances (peat, lignite, and coal) [15–21], agricultural wastes (peanut hull, citrus waste, banana peel, and rice husk) [22–25] and forestry wastes (bark, cone, and sawdust) [26–28].

Biosorption processes are characterized by high efficiency, no formation of toxic and harmful by-products, rapid kinetics, selectivity, and the possibility of recovering contaminants and reuse of the adsorbent. Moreover, in cases when regeneration is not efficient and the loaded material is not hazardous, it may be discarded or incinerated [9,20,29,30].

Peat is a young Quaternary, mainly Holocene, organogenic sedimentary rock at the first stage of coalification, formed through decomposition of plant material in the presence of weakly acidic humic substances. Peat composition depends on its age, the type of vegetation, the climate and the acidity of the water. Its main constituents are cellulose, lignin, humic substances (fulvic and humic acids) and mineral substances such as Fe(III) oxides-hydroxides and silica. Due to the presence of humic substances, peat is a porous material with a high specific surface area. Its surface contains polar functional groups such as carboxylic acids (–COOH), alcohols (–OH), and phenols (ph–OH), where alkaline and alkaline earth cations may be substituted for H<sup>+</sup>. Surface functional groups may be involved in bonding organic pollutants and heavy metals (cationic or anionic) [7,31] by various interactions such as ion exchange, hydrogen bonds and van der Waals forces [32,33]. Moreover, according to protonation or deprotonation reactions:



The surface of peat particles has a positive or negative charge, respectively. The surface charge allows the bonding of pollutants by electrostatic attractions. Due to its physical and chemical properties, low-moor peat has good sorption properties.

Besides peatlands, peat occurs also in the overburden of lignite deposits. During excavation, the overburden is dumped and then used to reclaim terrains devastated by mining [15].

In Poland, the price of peat (€24 per ton [34]) is incomparably lower than the price of activated carbon (from €2,700 per ton [35]), which is the most commonly used adsorbent in industry. Therefore, peat can be considered as a low-cost adsorbent for the treatment of wastewater to make the adsorption process economically feasible.

Research on the adsorption capacity of low-moor peats for dyes has been carried out for many years, but most of it has concerned adsorption from dye solutions based on distilled or tap water without taking into account the auxiliaries present in textile wastewater. Studies on the effect of real conditions on the adsorption process are usually carried out in the presence of NaCl, as wastewater from the textile industry contains large amounts [1,36]. The results of the studies show that the presence of salts in solution may affect adsorption capacities because they increase ionic strength and can change the properties of the adsorbent and adsorbate, as well as the aggregation of dye molecules in solution [36,37]. Sepulveda and Santana [1] explain the increase in Acid Black 1 adsorption in the presence of NaCl by reduction in the repulsive interactions between dye molecules and the peat surface in the presence of Na<sup>+</sup> ions that neutralize carboxylic functional groups.

The effect of auxiliaries on the amount of adsorbed dyes depends on the adsorbent-dye-auxiliary substance system. Therefore, it was decided to determine the effect of selected, most frequently used auxiliary substances on the adsorption capacity of low-moor peat for selected reactive and acid dyes and their binding mechanism.

The aim of the study was to determine the adsorption capacity of peat in relation to anionic reactive dyes (Reactive Blue 19, Reactive Blue 81, Reactive Black 5) and acid dyes (Acid Black 1, Acid Blue 9) and to determine the effect of the auxiliary substances most frequently used in dyeing processes (NaCl, Na<sub>2</sub>CO<sub>3</sub>, and CH<sub>3</sub>COOH) on the amount and method of binding dyes on a low-moor peat occurring in the overburden of a lignite deposit (Bełchatów, Central Poland). Four adsorption isotherms, that is, three two-parameter isotherms (Freundlich, Langmuir, Dubinin–Radushkevich (D–R)) and one three-parameter isotherm (Sips) were used to interpret the results obtained. Parameters estimated by nonlinear regression allowed calculation of the maximum adsorption capacity and determination of the mechanism of dye binding.

## 2. Materials and methods

### 2.1. Adsorbent

Alder low-moor peat was collected from overburden mining of the Bełchatów Lignite Mine (Central Poland).

The peat sample was dried at room temperature ( $25^{\circ}\text{C} \pm 2^{\circ}\text{C}$ ) and then ground and sieved to a particle size below 0.5 mm, with no modifications. The adsorbent was stored in dry conditions until further use. The textural, physical and chemical properties of the peat can be found in our previous work [15] and the methods used in Kyzioł-Komosińska et al. [38].

The morphological and chemical analyses of the surface of the raw peat sample were performed on a scanning electron microscope (Field emission scanning electron microscopy (FESEM), Hitachi, Model: S-4700, Japan) equipped with an energy dispersive X-ray detector system (EDS).

Additionally, the samples of raw peat and peat loaded with two studied dyes – RB19 or ABk1 – and loaded with the dyes in the presence of 20%  $\text{CH}_3\text{COOH}$  solution at the maximum initial dye concentration were characterized by Fourier-transform infrared spectroscopy (FTIR) to identify the surface functional groups and their contribution to the binding of the dyes. Spectra of the studied samples were obtained using a Bruker Tensor 27 spectrometer (USA) in the range of  $4,000\text{--}400\text{ cm}^{-1}$ . Samples were prepared in the form of pellets (2 mg of the sample was ground in an agate mortar and homogenized with 180 mg of KBr). High-quality spectra were obtained by 256 scans at  $2\text{ cm}^{-1}$  resolution.

## 2.2. Dyes

Dyes selected for study were the following:

- *Reactive dyes*: Reactive Blue 19 (RB19) – CAS 2580-78-1, C.I. 61200; Reactive Blue 81 (RB81) – CAS 75030-18-1, C.I. 18245; and Reactive Black 5 (RBk5) – CAS 17095-24-8, C.I. 20505;
- *Acid dyes*: Acid Blue 9 (AB9) – CAS 2650-18-2, C.I. 42090; and Acid Black 1 (ABk1) – CAS 1064-48-8, C.I. 20470.

They were produced by Boruta Zachem-Kolor, Ltd., (Poland).

The chemical structures of the dyes, their properties, and wavelengths at which the absorbance was measured are shown in Table 1.

## 2.3. Auxiliary substances

The effect of auxiliary substances on dye adsorption was investigated by the addition of:

- 5% NaCl solution – the pHs of dye solutions were 5.4 for RB19, 5.3 for RB81 and 4.65 for RBk5,
- 10%  $\text{Na}_2\text{CO}_3$  solution – the pH of dye solutions was 9.2,
- 20%  $\text{CH}_3\text{COOH}$  solution – the pH of reactive dyes solutions was 3.2 and for acid dyes 3.0 and 4.6.

## 2.4. Adsorption capacity studies

The adsorption of reactive and acid dyes onto peat and studies on the effect of auxiliary substances were carried out in static conditions using a batch method at room temperature. The stock solutions were prepared by dissolving 1 g of dye in 1,000 mL of distilled water. The working dye solutions (from 1 to 1,000  $\text{mg L}^{-1}$ ) were prepared by diluting the stock solution with distilled water. The pH values of the working

solutions were natural, without pH adjustment. Control experiments without peat were carried out for all dye solutions to ascertain that the adsorption of dyes did not take place on the walls of the containers.

The adsorbent dose was  $50\text{ g L}^{-1}$ , that is, the solid phase to solution ratio was 1:20. The prepared suspensions were agitated on a horizontal shaker (the intensity of agitation was 2 rps) for 24 h to reach equilibrium and the solution separated from the solid phase using filter papers. Initial and equilibrium dye concentrations were determined using ultraviolet-visible spectrophotometry (Varian Cary 50 scan spectrophotometer, 1 cm cell) at wavelengths given in Table 1. By referring to the calibration curves of the dyes, the corresponding concentrations in the equilibrium solutions were obtained. Dilutions were carried out when the measurement exceeded the linearity of the calibration curve.

The pH in the equilibrium solutions was measured by a potentiometric method using a glass electrode (ERH-111, Hydromet, Poland).

The amount of dye adsorbed and the removal efficiency were calculated using the following equations:

$$q = \frac{(C_0 - C_{\text{eq}}) \times V}{m \times 1,000} \text{ (mg g}^{-1}\text{)} \quad (3)$$

$$\text{RE} = \frac{(C_0 - C_{\text{eq}})}{C_0} \times 100\% \quad (4)$$

where  $q$  – amount of dye adsorbed onto peat ( $\text{mg g}^{-1}$ ), RE – removal efficiency (%),  $C_0$  – initial dye concentration ( $\text{mg L}^{-1}$ ),  $C_{\text{eq}}$  – equilibrium dye concentration ( $\text{mg L}^{-1}$ ),  $V$  – volume of the solution (mL),  $m$  – mass of the adsorbent (g).

All adsorption samples were studied in duplicate and the mean values used.

## 2.5. Adsorption isotherms

According to Rangel-Porras et al. [39], two methods can be used to study the behavior of adsorption isotherms:

- identification by the type of the isotherm shape according to Giles classification; namely, C, L and S isotherms [40], and
- application of formulated mathematical models to describe adsorption behavior.

Three two-parameter adsorption isotherms (Freundlich, Langmuir, D–R) and one three-parameter isotherm (Sips) were used to explain equilibrium adsorption. These are conventional and are the most frequently used models in the description of adsorption processes. The parameters estimated from selected models provide some insights into the mechanism of the adsorption process, the surface properties and the affinity of the adsorbent [41].

The Freundlich isotherm:

$$q = K_F \times C_{\text{eq}}^{\frac{1}{n_F}} \quad (5)$$

Table 1  
 Characteristics of reactive and acid dyes

| Dye  | Chemical structure | Molar mass<br>(g mol <sup>-1</sup> ) | pH (H <sub>2</sub> O) | λ (nm) | Number of<br>donors | Number of<br>acceptors |
|------|--------------------|--------------------------------------|-----------------------|--------|---------------------|------------------------|
| RB19 |                    | 626.5                                | 4.29                  | 595.9  | 3                   | 12                     |
| RB81 |                    | 808.0                                | 4.97                  | 584.0  | 3                   | 17                     |
| RBk5 |                    | 995.8                                | 4.53                  | 584.0  | 3                   | 22                     |
| ABk1 |                    | 618.5                                | 7.95                  | 619.0  | 3                   | 14                     |
| AB9  |                    | 768.9                                | 6.09                  | 630.0  | 0                   | 10                     |

where  $K_f$  – Freundlich equilibrium constant related to the adsorption capacity and adsorption intensity of the system ( $\text{mg g}^{-1} (\text{L mg}^{-1})^{1/n_f}$ ),  $1/n_f$  – expresses favorability of adsorption (dimensionless), is the empirical model that describes adsorption on heterogeneous surfaces. This model assumes that the concentration of the adsorbate on the adsorbent surface increases with the adsorbate concentration [41,42].

The parameter  $1/n_f$  is a measure of surface heterogeneity, which becomes more heterogeneous as its value gets closer to zero [43]. According to Brown et al. [44] the value of  $1/n_f < 1$  implies a favorable nature of adsorption;  $1/n_f > 1$ , cooperative adsorption; and  $1/n_f = 1$ , linear adsorption.

The Langmuir isotherm:

$$q = \frac{q_{\max} K_L C_{\text{eq}}}{1 + K_L C_{\text{eq}}} \quad (6)$$

where  $q_{\max}$  – maximum adsorption capacity ( $\text{mg g}^{-1}$ ),  $K_L$  – Langmuir constant related to the affinity of the binding sites and the energy of adsorption ( $\text{L mg}^{-1}$ ), assumes monolayer adsorption at a fixed number of well-defined sites that are energetically equivalent, with no interactions between the adsorbate molecules [41,45]. It allows estimation of the maximum adsorption capacity of the adsorbent.

A dimensionless constant, the separation factor  $R_L$  can be calculated from the Langmuir model:

$$R_L = \frac{1}{1 + K_L C_0} \quad (7)$$

The value of the parameter  $R_L$  indicates the shape of isotherm:  $R_L > 1$ , the adsorption is unfavorable;  $R_L = 1$ , the adsorption is linear;  $0 < R_L < 1$ , the adsorption is favorable;  $R_L = 0$ , the adsorption is irreversible [46].

The D–R isotherm:

$$q = q_D \times \exp(-\beta \varepsilon^2) \quad (8)$$

where  $q$  – amount of dye adsorbed per unit mass of the adsorbent ( $\text{mmol g}^{-1}$ ),  $q_D$  – theoretical saturation capacity ( $\text{mmol g}^{-1}$ ),  $\beta$  – constant related to the adsorption energy ( $\text{mol}^2 \text{kJ}^{-2}$ ),

$$\varepsilon = RT \ln \left( 1 + \frac{1}{C_{\text{eq}}} \right) \quad (9)$$

$\varepsilon$  – Polanyi potential,  $R$  – gas constant ( $\text{J mol}^{-1} \text{K}^{-1}$ ),  $T$  – temperature (K), is an empirical model that describes adsorption with a Gaussian energy distribution onto a heterogeneous surface [43,46,47].

The constant  $\beta$  gives the mean free energy ( $E$ ) of adsorption per molecule of the adsorbate:

$$E = \frac{1}{\sqrt{2\beta}} \quad (10)$$

If the value of  $E$  is between 8 and 16  $\text{kJ mol}^{-1}$ , the adsorption is a chemical process, whereas if the value is lower than 8  $\text{kJ mol}^{-1}$ , the adsorption process is of a physical nature [46].

The Sips isotherm:

$$q = \frac{q_{\max} K_s C_{\text{eq}}^{1/n_s}}{1 + K_s C_{\text{eq}}^{1/n_s}} \quad (11)$$

where  $q_{\max}$  – Sips maximum adsorption capacity ( $\text{mg g}^{-1}$ ),  $K_s$  – Sips constant related with affinity constant ( $(\text{L mg}^{-1})^{1/n_s}$ ),  $1/n_s$  – Sips exponent which represents the surface heterogeneity (dimensionless), is a three-parameter empirical model. It is a combination of the Langmuir and Freundlich isotherms used to predict adsorption on heterogeneous surfaces. At low adsorbate concentrations, it is reduced to the Freundlich isotherm and at high concentrations the equation is transformed into the Langmuir isotherm, predicting monolayer adsorption [41,48].

The nonlinear parameters in the isotherm equations were estimated using Statistica 9.0, and the Levenberg–Marquardt algorithm was applied. The estimated parameters allowed determination of the mechanism of dye binding and the maximum adsorption capacity. To evaluate the goodness of fit of the isotherm models to the data, the coefficient of determination ( $R^2$ ) as well as three error functions, measuring the differences between the experimental and the calculated data, were applied [34,43,49]. The sum of the squares of the errors (SSE):

$$\sum_{i=1}^n (q_{\text{cal}} - q_{\text{exp}})_i^2 \quad (12)$$

Residual root mean square error (RMSE):

$$\sqrt{\frac{1}{n-2} \sum_{i=1}^n (q_{\text{exp}} - q_{\text{cal}})_i^2} \quad (13)$$

Nonlinear chi-square test  $\chi^2$ :

$$\sum_{i=1}^n \frac{(q_{\text{exp}} - q_{\text{cal}})_i^2}{q_{\text{cal}}} \quad (14)$$

where  $q_{\text{cal}}$  – calculated value of adsorption capacity,  $q_{\text{exp}}$  – experimental value of adsorption capacity,  $n$  – the number of observations in the experimental data.

High values of  $R^2$  (close to 1) and low values of SSE, RMSE and  $\chi^2$  indicate similarity of the values calculated based on models to those obtained experimentally and a good fit of the isotherm to the experimental data [43,49].

### 3. Results and discussion

#### 3.1. Properties of peat

The main physicochemical properties of peat determining its adsorption capacity are presented in Table 2.

Table 2  
Physicochemical properties of low-moor Alder peat

| Properties   | Values                    |       |
|--|---------------------------|-------|
| Total (H <sub>2</sub> O)/external (N <sub>2</sub> ) surface area - SSA (m <sup>2</sup> g <sup>-1</sup> ) | 218.9/11.38               |       |
| Total porosity (%)   | 0.520                     |       |
| Pore size distribution (%)   | Macropores $d > 50$ nm    | 35.65 |
|  | Mesopores $50 > d > 2$ nm | 62.37 |
|  | Micropores $d < 2$ nm     | 1.98  |
| pH (H <sub>2</sub> O)/pH <sub>pzc</sub>  | 5.62/5.77                 |       |
| Cation exchange capacity (cmol <sub>(+)</sub> kg <sup>-1</sup> )   | 125                       |       |
| Functional groups content (cmol <sub>(+)</sub> kg <sup>-1</sup> )  | -OH                       | 115.3 |
|  | -COOH                     | 90    |

The degree of alder low-moor peat decomposition was 70% and the ash content was 20.88%. The main components of the mineral fraction of the studied peat were SiO<sub>2</sub> (8.26%), CaO (4.57%), Al<sub>2</sub>O<sub>3</sub> (2.32%), and Fe<sub>2</sub>O<sub>3</sub> (2.31%). Iron occurred mainly in free non-crystalline form and surface coating material of other particles as (hydr)oxides as well as bound to organic matter [15]. Average chemical composition computed for raw peat surface with the use of the point analysis from scanning electron microscopy equipped with an EDS was as follows: SiO<sub>2</sub> 10.05% ± 2.11%; CaO 4.98% ± 1.22%; Al<sub>2</sub>O<sub>3</sub> 3.21% ± 0.89%; and Fe<sub>2</sub>O<sub>3</sub> 12.98% ± 1.91%. The high content of Fe<sub>2</sub>O<sub>3</sub> on the peat surface suggests that Fe compounds can modify the peat surface and provide additional sorption centers. The total specific surface area of the peat was 218.9 m<sup>2</sup> g<sup>-1</sup> and the external surface area was 11.38 m<sup>2</sup> g<sup>-1</sup>, high total porosity – approximately 0.520 with mesopores and macropores as the dominant pore size (Table 2, Fig. 1).

Cation exchange capacity was 125 cmol<sub>(+)</sub> kg<sup>-1</sup>, with Ca<sup>2+</sup> and H<sup>+</sup> being the main exchangeable cations. The value of pH of peat in water solution was 5.62. The point of zero charge (pH<sub>pzc</sub>) was 5.77 and indicated that at a solution pH lower than 5.77 the surface of the peat particles was positively charged and adhered negatively charged pollutants; at a solution pH greater than 5.77 the surface was negatively charged and bound positively charged pollutants. The quantitative analysis showed that the main, acid functional groups were -COOH (90 cmol<sub>(+)</sub> kg<sup>-1</sup>) and -OH

(115.3 cmol<sub>(+)</sub> kg<sup>-1</sup>) (Table 2) in which the H<sup>+</sup> ions may be substituted by Ca<sup>2+</sup>.

### 3.2. Surface functional groups in studied peat

Normalized FTIR spectra of peat before and after adsorption of two studied dyes – RB19 or ABk1 – are shown in Fig. 2. The spectra of the peat showed the presence of transmission bands specific for humic substance structures (humic and fulvic acids) [50]. FTIR spectra of the peat showed a broad peak at 3,600–3,000 cm<sup>-1</sup> with a maximum at 3,410 cm<sup>-1</sup>. This peak can be attributed to the O–H stretching of phenols and carboxyl groups, as well as N–H stretching groups of amines and, can show intermolecular and intramolecular H-bonds. Two peaks, at 1,620 and 1,380 cm<sup>-1</sup>, originated from the symmetric and anti-symmetric stretching vibration of the COO group and indicated that carboxyl groups are either dissociated (COO) or forming a complex with a metal ion (COO–Me) [51]. Moreover, the absence of a peak at 1,700 cm<sup>-1</sup> and the presence of a 1,380 cm<sup>-1</sup> peak confirm that carboxyl groups in peat are found in their dissociated form (COO). The band at 1,410 cm<sup>-1</sup> originated from C–C stretching vibrations in the aromatic rings or C–H<sub>2</sub> bending, and the band at 1,220 cm<sup>-1</sup> can be attributed to C–O stretching and O–H deformation in COOH groups. The peaks at 1,030 cm<sup>-1</sup> and

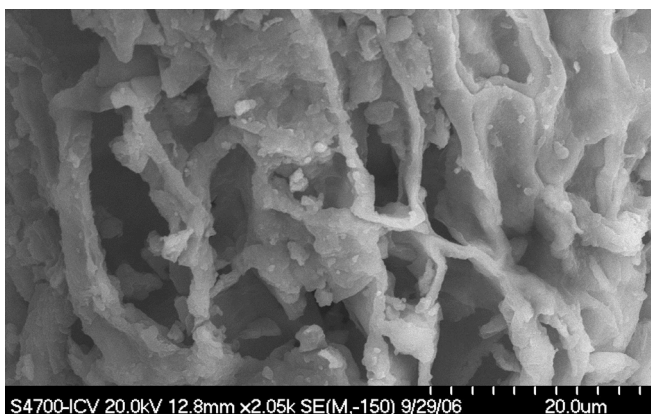


Fig. 1. Scanning electron microscopy of the peat sample.

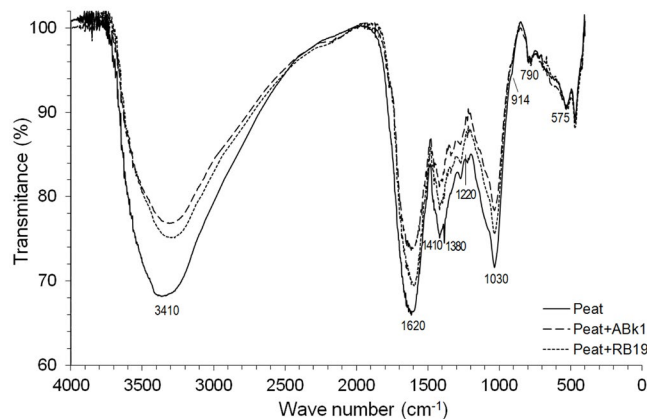


Fig. 2. FTIR spectra of the raw peat and peat loaded with the dyes.

914  $\text{cm}^{-1}$  correspond to the C–O and O–H stretching vibrations in polysaccharides and alcohols, and/or may correspond to silicate impurities. Moreover, the broad peaks at 3,600–3,000  $\text{cm}^{-1}$  and the strong peak at 1,620  $\text{cm}^{-1}$  can be attributed to the O–H stretching vibration of water and hydrated species on the iron (hydr)oxide surface, whereas those at 575, ~800, and ~900  $\text{cm}^{-1}$  correspond to the Fe–O, and Fe–OH vibrations [52].

3.3. Adsorption of reactive dyes and the effect of auxiliary substances on the adsorption capacity

The curves of adsorption of reactive dyes on peat in the system  $q = f(C_{\text{eq}})$  and the removal efficiency from the solution – in the system  $\text{RE} = f(C_0)$  and a pH in the equilibrium solutions as  $\text{pH} = f(C_{\text{eq}})$  are shown in Figs. 3 and 4, respectively.

In the low initial concentration range (1–5  $\text{mg L}^{-1}$ ), reactive dyes were bound completely. Various affinity of dyes to the peat surface occurred at initial concentrations above 10  $\text{mg L}^{-1}$ . The removal efficiency of reactive dyes decreased in the following order RB19 > RB81 > RBk5 and was 99.23%–69.45%, 93.75%–57.18% and 92.67%–25.58%, respectively. The experimental maximum adsorption capacities of peat for reactive dyes at an initial dye concentration of 1,000  $\text{mg L}^{-1}$  were found to be 14.15, 11.6, and 5  $\text{mg g}^{-1}$ , respectively. According to Giles classification [40], the adsorption isotherms of reactive dyes were of the L-type, which indicates a high affinity of the dyes to the surface at low concentrations, decreasing with increasing initial concentration.

Reactive dyes were anionic and of different molecular diameters (RB19,  $d = 1.87 \text{ nm}$ ; RB81,  $d = 1.94 \text{ nm}$ ; RBk5,  $d = 3.02 \text{ nm}$ , the diameters determined using ChemBio3D Ultra), the number of acceptors and the number of donors (Table 1). The obtained results indicate that the adsorption of reactive dyes depended on the number of acceptor groups and the size of the dye molecule. The adsorption capacity of peat decreased with an increasing number of acceptor groups. Our previous study [15] showed a strong relationship between the adsorption capacity of low-moor peats and the ratio of the number of hydrogen atom donors to the

number of hydrogen atom acceptors in the dye functional groups. A significant peat porosity with the dominance of mesopores ( $50 > d > 2 \text{ nm}$ ) and macropores ( $d > 50 \text{ }\mu\text{m}$ ) (Table 2) indicates that the dyes can bind in the peat pores. Dye RB19 was bound in the largest amount due to its lowest molecular weight and diameter, which facilitated the mobility and diffusion of the dye into the pores. Dye RBk5, with the highest molecular weight and diameter, was bound in the smallest amount.

Despite the acidity of the dyes RB19, RB81 and RBk5 (pH 4.29–4.97), the pH in the equilibrium solution varied, at 5.20–5.90, 5.92–6.11, and 6.24–6.45, respectively (Fig. 4). The pH values were close to or higher than the pH of peat (pH 5.62, Table 2) due to its high buffer capacity [53]. The structure of reactive dyes and the presence of –OH, =NH, –NH and –SO<sub>3</sub> groups indicate that they could be bound with surface groups of humic acids (–COOH and –OH) by hydrogen bonds as well as van der Waals forces and  $\pi$ – $\pi$  interactions (Fig. 5) [14,54].

The comparison of the pH values in the equilibrium solutions with the point of zero charge of peat ( $\text{pH}_{\text{pzc}} 5.77$ ,

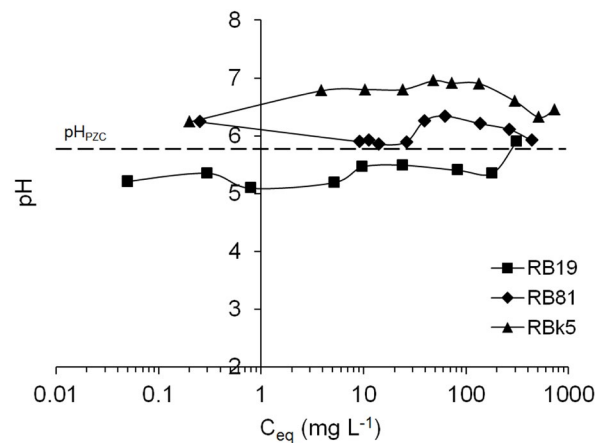


Fig. 4. pH values in the equilibrium solutions for reactive dyes.

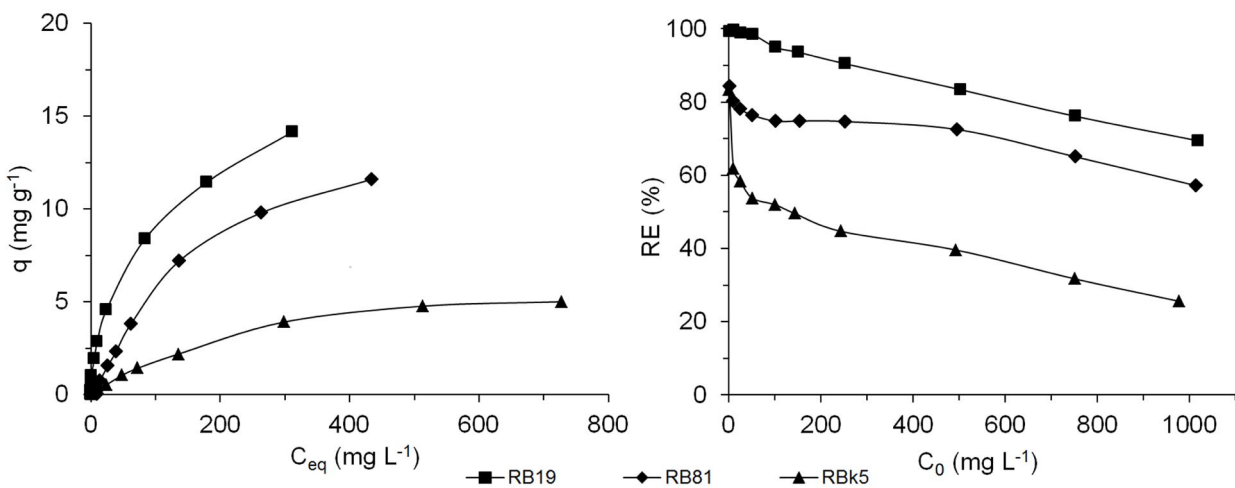


Fig. 3. Equilibrium adsorption isotherms and the removal efficiency of reactive dyes.

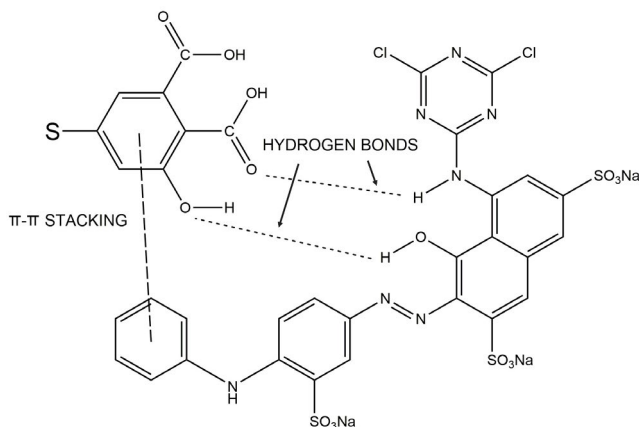
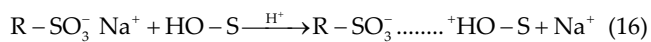
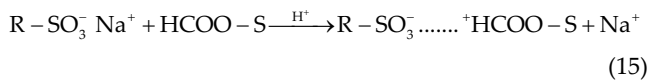


Fig. 5. Intermolecular interactions between dye groups and peat surface groups.

Table 2) showed that only adsorption of RB19 dye occurred at  $\text{pH} < \text{pH}_{\text{PZC}}$  over the whole range of initial concentrations (Fig. 4). This indicates that the peat surface was positively charged according to Reaction 1 and this dye may be bound also as a result of electrostatic interactions, according to the reactions:



where S – surface of peat.

On the other hand, dyes RB81 and RBk5 were bound at  $\text{pH} > \text{pH}_{\text{PZC}}$ , that is, to a negatively charged surface, so they cannot be bound by electrostatic interactions.

The effect of NaCl (at concentration of 5%) and  $\text{Na}_2\text{CO}_3$  (at concentration of 10%) ( $\text{pH}$  5.4 for RB19, 5.3 for RB81, 4.65 for RBk5 and  $\text{pH}$  9.2, respectively) as well as  $\text{CH}_3\text{COOH}$  (at concentration of 20% and  $\text{pH}$  3.2) on the adsorption capacity of peat in relation to reactive dyes RB19, RB81 and RBk5 and on their removal efficiency is shown in Fig. 6, and on the  $\text{pH}$  changes in the equilibrium solutions – in Fig. 7.

It was observed that in the presence of all auxiliaries used the adsorption capacity of peat for reactive dyes increased over the whole range of initial concentrations and depended on the dye-auxiliary substance system.

It was also observed that the lower the peat's ability to bind dyes, the greater the effect of auxiliaries. The effect of NaCl,  $\text{Na}_2\text{CO}_3$ , and  $\text{CH}_3\text{COOH}$  on RB19 adsorption was the smallest and appeared at dye concentrations above  $250 \text{ mg L}^{-1}$  (Fig. 6). In the presence of the auxiliary substances, the adsorption of the dye increased by 9.52%–29.87%, 12.0%–28.67% and 9.20%–22.06%, respectively, to maxima of 18.32, 17.26, and  $18.20 \text{ mg g}^{-1}$ , respectively. The removal efficiency varied between 99.5%–90.77%, 97%–85.2% and 99%–87.68%, respectively. In the presence of auxiliaries, the adsorption of RB19 occurred at  $\text{pH}$  6.65–6.48, 7.35–7.59, and 4.82–4.87, respectively. The addition of salts increased the  $\text{pH}$  values in the equilibrium solutions, whereas in the presence of

acetic acid the adsorption occurred at  $\text{pH} < \text{pH}_{\text{PZC}}$  of peat and the  $\text{pH}$  remained constant (Fig. 7).

The removal efficiency of RB81 in the presence of auxiliaries NaCl,  $\text{Na}_2\text{CO}_3$  and  $\text{CH}_3\text{COOH}$  was high and varied at 99.51%–97.68%, 93%–76.68%, and 99.07%–92.2%, respectively (Fig. 6). The adsorption capacity of peat for RB81 dye increased by 33.3%–69.75%, 24.7%–36.82%, and 32.1%–58.17%, respectively, to maxima of 19.69, 15.82, and  $18.35 \text{ mg g}^{-1}$ , respectively. The adsorption of RB81 in the presence of NaCl and  $\text{Na}_2\text{CO}_3$  occurred in the  $\text{pH}$  range of 5.68–5.31 and 5.62–6.17, respectively, close to the  $\text{pH}$  of peat. The  $\text{pH}$  values of the equilibrium solution with the addition of acid were below  $\text{pH}_{\text{PZC}}$  and ranged between 4.92 and 4.63 (Fig. 7). After the addition of NaCl and  $\text{CH}_3\text{COOH}$ , the shape of the adsorption isotherm of RB81 changed from the L-type to the H-type, which means that the affinity of the peat surface for the dye increased.

The highest increase in the adsorption was observed for RBk5 over the whole range of initial concentrations. In the presence of auxiliary substances NaCl,  $\text{Na}_2\text{CO}_3$ ,  $\text{CH}_3\text{COOH}$ , the adsorption capacity of peat for RBk5 increased by 57%–136%, 51%–221% and 40%–93.4%, respectively. The dye was removed at levels of 93.4%–58.28%, 96%–78.98% and 84.62%–46.32%, respectively. At the maximum initial concentration of RBk5, adsorption was 11.82, 16.65, and  $9.67 \text{ mg g}^{-1}$ , respectively (Fig. 6).

A comparison of the  $\text{pH}$  values in the equilibrium solutions with the point of zero charge of peat showed that in the presence of  $\text{CH}_3\text{COOH}$  the adsorption of RBk5 dye proceeded at  $\text{pH} < \text{pH}_{\text{PZC}}$  to a positively charged surface. The functional groups on the surface of peat are protonated by  $\text{H}^+$  ions present in the solution and, thus, anionic dyes can also be bound by electrostatic interactions, which increase the adsorption.

According to Ip et al. [14] the presence of salts in solution can affect the adsorption process: the addition of salts will increase the adsorption capacity when the electrostatic interaction between the dye molecules and the adsorbent surface is repulsive, whereas when the electrostatic interaction is attractive, salts will decrease the adsorption capacity of the system. The positive and negative ions in the salts can neutralize charge on the adsorbent surface and the charged dye molecules and reduce the electrostatic interactions between them.

The adsorption of dye RB19 with added salts NaCl and  $\text{Na}_2\text{CO}_3$  and the adsorption of RBk5 and RB81 dyes with added  $\text{Na}_2\text{CO}_3$  occurred at  $\text{pH} > \text{pH}_{\text{PZC}}$ , which proves the positive effect of the added salts when the electrostatic interactions are repulsive. The adsorption of dyes RB81 and RBk5 with added NaCl proceeded at  $\text{pH} < \text{pH}_{\text{PZC}}$  and, according to the theoretical assumptions, the addition of NaCl should decrease the adsorption capacity. However, the obtained results indicate that the adsorption capacity of peat increased. Al-Degs et al. [55] obtained similar results during the tests of the adsorption of reactive dyes on activated carbon. The authors suggested that the increase in the adsorption capacity after NaCl addition could be attributed to the dimerization of the reactive dye molecules in solution. The increase in aggregation can be explained by the fact that the presence of salt ions increases the intermolecular forces causing the aggregation, including van der Waals, ion-dipole and dipole-dipole forces.

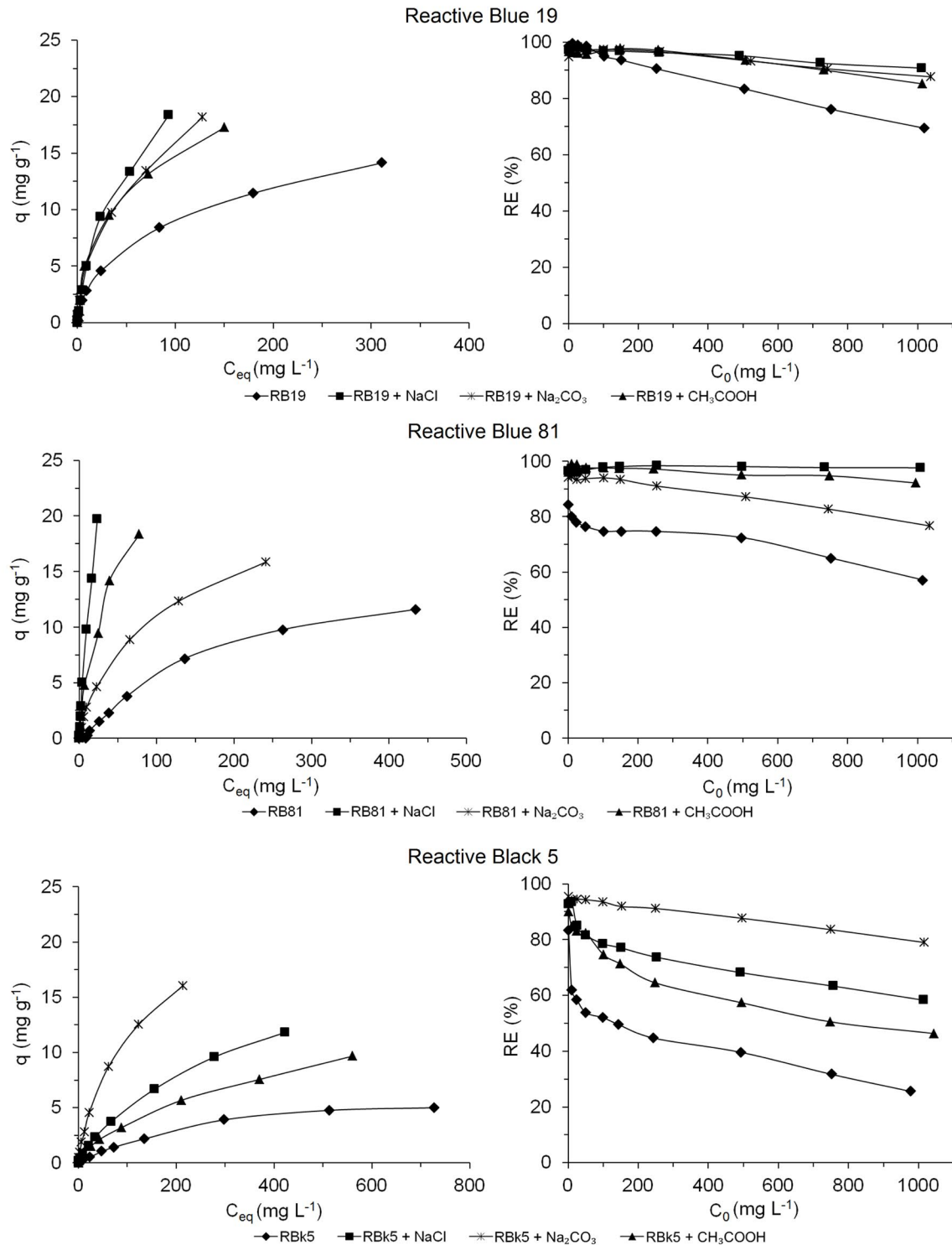


Fig. 6. Equilibrium adsorption isotherms of reactive dyes on peat in the presence of auxiliary substances and their removal efficiency.

An increase in the adsorption capacity of peat to reactive dyes after adding NaCl was also observed by Ip et al. [14] and Sepulveda et al. [3]. According to Ip et al. [14], the adsorption of RBk5 onto peat in the presence of 0.1 M NaCl at an initial dye concentration of 1,000 mg L<sup>-1</sup> increased 5.5-fold, from 5.44 to 29.82 mg g<sup>-1</sup>. A much stronger effect of NaCl than we

had observed may have been caused by the higher concentration of NaCl used. In the studies by Sepulveda et al. [3] on four reactive dyes (Yellow CIBA WR 200%, Dark Blue CIBA WR, Navy CIBA WB and Red CIBA WB 150%), in the presence of NaCl solution of ionic strength 0.1 M, the sorption onto peat was from two to three times higher. The authors

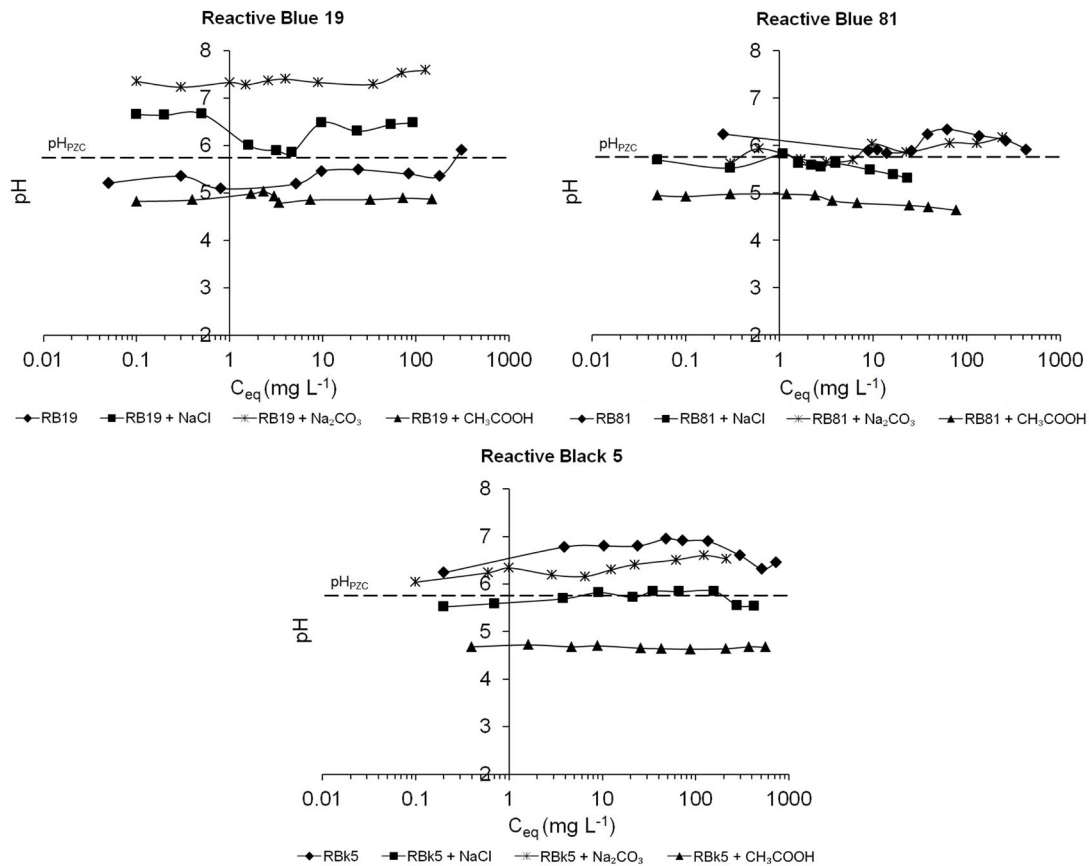


Fig. 7. Effect of auxiliary substances on the pH values in the equilibrium solutions for reactive dyes.

explain the increase in the adsorption capacity in the presence of NaCl ions by the fact that the repulsive electrostatic interactions between the peat surface and dye molecules had been reduced.

#### 3.4. Adsorption of acid dyes and the effect of auxiliary substances on the adsorption capacity

The equilibrium adsorption isotherms for acid dyes ( $q = f(C_{eq})$ ) and the removal efficiency ( $RE = f(C_0)$ ) are presented in Fig. 8; the pHs of the equilibrium solutions ( $pH = f(C_{eq})$ ) are shown in Fig. 9.

The studied acid dyes, ABk1 and AB9, are alkaline or weakly acidic, respectively (Table 1) and showed different affinities for the peat surface. Dye ABk1 was removed from the solution at levels of 99–90.34% over the whole range of initial concentrations (1–1,000 mg L<sup>-1</sup>). The maximum adsorption capacity was 17.67 mg g<sup>-1</sup>. Dye AB9 showed a very low affinity for the peat surface. The dye was removed from the solution in the range 95%–32.94% and the maximum adsorption capacity was 6.67 mg g<sup>-1</sup>. The adsorption isotherm of ABk1 can be classified as type *H* and that of AB9 as type *S* according to Giles classification. The *H*-type isotherm indicates the high affinity of ABk1 dye for the peat surface, and the *S*-type isotherm indicates a low affinity of AB9 for the peat surface at low dye concentrations, which increases with the initial concentration.

The adsorption of ABk1 and AB9 occurred at pH values in the ranges of 6.67–6.96 and 6.24–6.08, respectively, that is, at  $pH > pHPZC$  indicating a negative surface charge. Dye ABk1 could be bound by peat as a result of hydrogen bonds between the dye functional groups –OH, –NH<sub>2</sub> (Table 1) and the ph–OH and –COOH groups of peat (Fig. 5).

Dye AB9 is an inner salt with a positive charge, which allows the formation of electrostatic interactions with a negatively charged surface. However, the adsorption of AB9 was much lower than the adsorption of ABk1, which may be related to the lack of donor groups in its structure (Table 1) and also to the larger size of the molecule in comparison with the ABk1 molecule (molecular diameters: ABk1,  $d = 2.03$  nm; AB9,  $d = 2.46$  nm), which hinders the transport of AB9 dye into the peat pores.

Two solutions of CH<sub>3</sub>COOH, of pHs of 3.0 and 4.6, were used to study the effect of auxiliary substances on the adsorption capacity of peat for acid dyes, as this acid is used for pH adjustment in the dyeing of natural fibers with acid dyes.

In the presence of CH<sub>3</sub>COOH at pH 3.0, ABk1 was removed from the solution at levels of 99%–97.86%, and the adsorption capacity increased by 1.2%–11% to a maximum of 19.65 mg g<sup>-1</sup> (Fig. 10). The adsorption occurred at pH 4.25–4.09 to a positively charged peat surface during the process. Under these conditions, the dye may also be bound by electrostatic forces, which increase the effectiveness of its removal from the solution. On the other hand, an increase

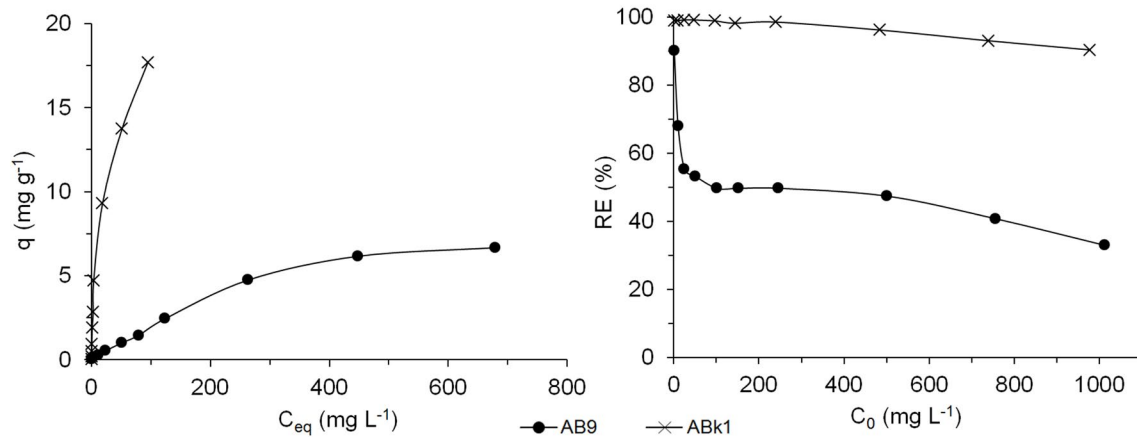


Fig. 8. Equilibrium adsorption isotherms of acid dyes onto peat and their removal efficiency.

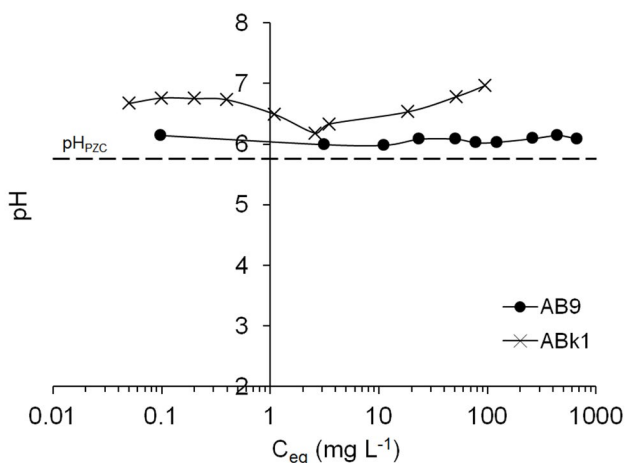


Fig. 9. pH values in the equilibrium solutions for acid dyes.

in the pH of  $\text{CH}_3\text{COOH}$  to 4.6 caused a decrease in ABk1 dye adsorption, especially at high initial concentrations ( $>250 \text{ mg L}^{-1}$ ). The dye was removed at 95%–79.5% with a maximum adsorption capacity of  $16.5 \text{ mg g}^{-1}$ , indicating a decrease in adsorption by 6.6%. There was also a change in adsorption isotherm shape from *H*-type to *L*-type. The pH values in the equilibrium solutions were in the range of 5.58–6.87 (Fig. 11) indicating a negative peat surface charge at initial concentrations  $>500 \text{ mg L}^{-1}$ . Comparing the adsorption curve (Fig. 10) with the pH curve in the equilibrium solution (Fig. 11), at initial concentrations of ABk1 in solution of  $>500 \text{ mg L}^{-1}$ , a change in the peat surface charge and a decrease in the adsorption, when compared to the dye without  $\text{CH}_3\text{COOH}$  can be noticed.

A similar effect of the addition of  $\text{CH}_3\text{COOH}$  on the adsorption of AB9 dye was observed. Depending on the pH of the acid (3.0 or 4.6), the dye was removed from the solution in the range of 99%–42.35% or 95%–18.81%, respectively. The adsorption increased by 24% to  $8.3 \text{ mg g}^{-1}$  or decreased by 43% to  $3.78 \text{ mg g}^{-1}$ , respectively. The increase in the adsorption in the presence of  $\text{CH}_3\text{COOH}$  of pH 3.0 caused a change in the shape of the adsorption isotherm according

to Giles' classification from an *S*-type to an *L*-type (Fig. 10). The adsorption proceeded at a pH in the ranges 4.31–4.25 and 6.16–6.0, respectively. This means that the lower the pH of the acid, the more effective its impact on the change in the peat surface charge.

The pH values of the equilibrium solutions indicate that the adsorption of acid dyes from the solutions at pH 3.0 occurred at pHs below the  $\text{pH}_{\text{pZC}}$  of peat (pH 5.77). The presence of  $\text{H}^+$  ions in the solution under acidic conditions caused protonation of the peat functional groups [56], so that the surface was positively charged and anionic acid dyes could also be bound to the peat surface as a result of electrostatic interactions, increasing the adsorption capacity of the material. Sepulveda and Santana [1] showed that the adsorption of acid dyes depends on the pH. The authors observed that the adsorption of Acid Black 1 on peat decreased with increasing pH from 2.0 to 8.0, with the highest decrease in the adsorption capacity from  $17.86$  to  $2.36 \text{ mg g}^{-1}$  at the change in pH from 2.24 to 5.3, when the pH was lower than the  $\text{pH}_{\text{pZC}}$  of peat. Similarly, the studies by Janos et al. [57] on the adsorption of Acid Black 26 and Acid Orange 7 on oxihumolite indicated a 14-fold and about a 6-fold decrease, respectively, in the adsorption capacity of the material with an increase in pH from 1.0 to 5.0. According to the authors, this was attributed to the dissociation of some functional groups on the adsorbent surface, which increased the negative surface charge, thus hindering the adsorption of acid dyes. The results of adsorption of Reactive Red 120 on *Chara contraria* obtained by Celekli et al. [46] also show a decrease in the adsorption capacity (from about 50 to about  $15 \text{ mg g}^{-1}$ ) with an increase in pH from 1.0 to 9.0, while at above pH 8.0 the adsorption capacity remained practically unchanged, which is related to the  $\text{pH}_{\text{pZC}}$  value (7.9) of the biomass used.

### 3.5. FTIR spectra of the peat samples before and after dyes adsorption

The FTIR spectra of peat loaded with RB19 or ABk1 at an initial concentration of  $1,000 \text{ mg L}^{-1}$  compared to the spectrum of raw peat provide useful information on the role of the peat surface functional groups in dye binding (Fig. 2).

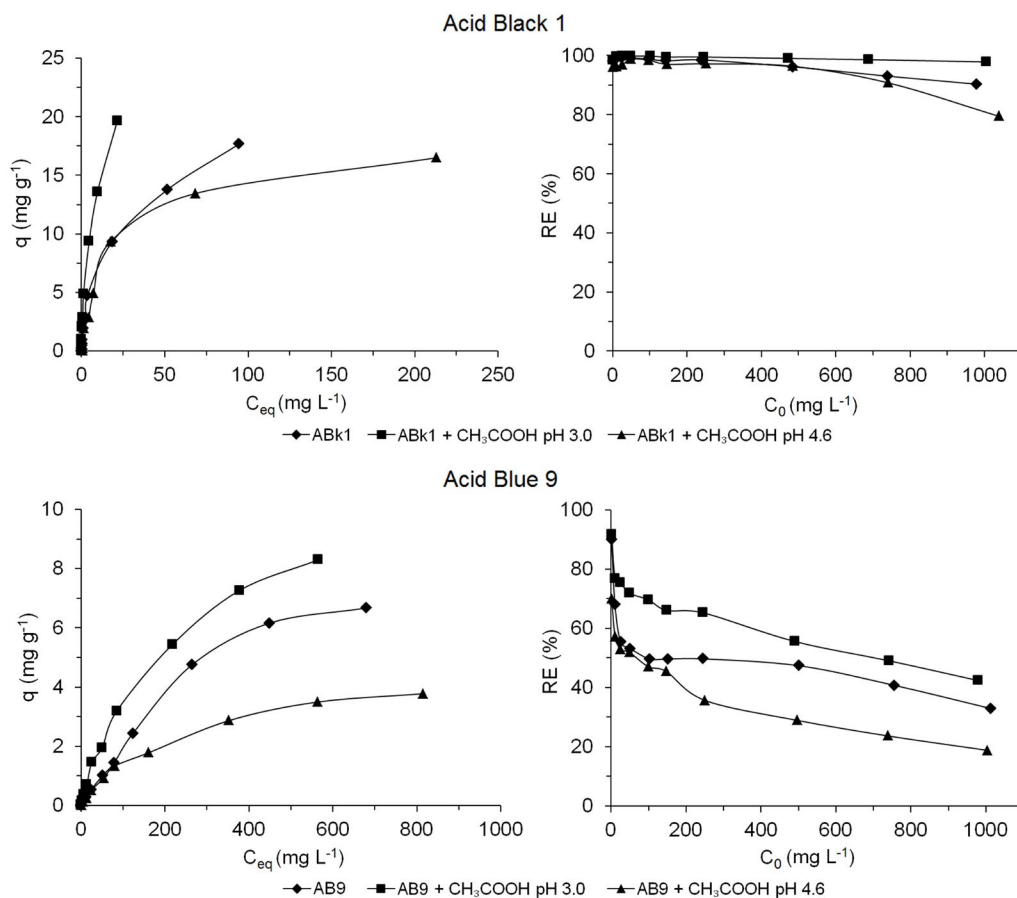


Fig. 10. Equilibrium adsorption isotherms of acid dyes on peat in the presence of auxiliary substances, and their removal efficiency.

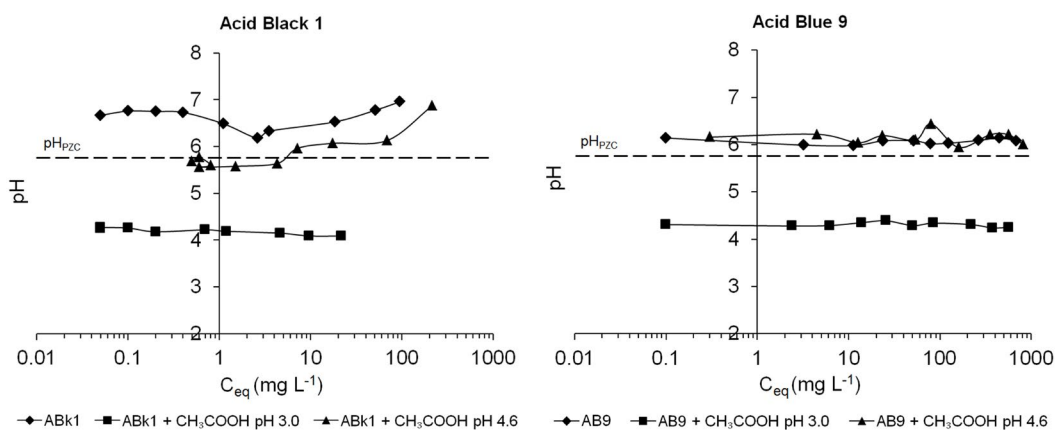


Fig. 11. Effect of  $\text{CH}_3\text{COOH}$  on the pH values in the equilibrium solutions for acid dyes.

Differences between the spectra in the region between 3,600 and 3,000  $\text{cm}^{-1}$ , and at 1,600; 1,380; and 1,030  $\text{cm}^{-1}$  were observed. Reduction in the peak intensities indicates the contribution of COOH, COO, and OH groups to the binding of dyes. Negative correlation (–) was observed between the intensity of peaks and the maximum peat sorption capacity for both dyes. Moreover, no changes in the spectra of

peat loaded with dyes and with the dyes in the presence of  $\text{CH}_3\text{COOH}$  are observed (omission the spectra of the peat after dyes adsorption in the presence of  $\text{CH}_3\text{COOH}$ ) and show a similar mechanism of dye binding.

Slight differences in peak intensities in the regions of 575, ~800, and ~900  $\text{cm}^{-1}$  may be due to the low contribution of iron oxides in the binding of these dyes or to the use of

Table 3  
Isotherm parameters, the values of the coefficient of determination and error functions for the adsorption of reactive dyes

|  | RB19     | +NaCl    | +Na <sub>2</sub> CO <sub>3</sub> | +CH <sub>3</sub> COOH | RB81     | +NaCl    | +Na <sub>2</sub> CO <sub>3</sub> | +CH <sub>3</sub> COOH | RBk5     | +NaCl    | +Na <sub>2</sub> CO <sub>3</sub> | +CH <sub>3</sub> COOH |
|--|----------|----------|----------------------------------|-----------------------|----------|----------|----------------------------------|-----------------------|----------|----------|----------------------------------|-----------------------|
| Freundlich isotherm  |          |          |                                  |                       |          |          |                                  |                       |          |          |                                  |                       |
| 1/n <sub>r</sub>   | 0.4513   | 0.5958   | 0.5418                           | 0.5018                | 0.6523   | 0.8813   | 0.5457                           | 0.5903                | 0.5588   | 0.6421   | 0.5793                           | 0.5951                |
| K <sub>r</sub> , mg g <sup>-1</sup> (L mg <sup>-1</sup> ) <sup>1/n<sub>r</sub></sup> | 1.082    | 1.250    | 1.336                            | 1.461                 | 0.2380   | 1.233    | 0.8279                           | 1.462                 | 0.1375   | 0.2499   | 0.7407                           | 0.2252                |
| R <sup>2</sup>   | 0.9978   | 0.9934   | 0.9935                           | 0.9765                | 0.9662   | 0.9921   | 0.9909                           | 0.9906                | 0.9760   | 0.9973   | 0.9946                           | 0.9988                |
| SSE  | 0.5137   | 2.395    | 2.359                            | 7.855                 | 5.610    | 3.298    | 2.612                            | 3.552                 | 0.8175   | 0.4343   | 1.584                            | 0.1197                |
| RMSE   | 0.06422  | 0.2994   | 0.2949                           | 0.9818                | 0.7012   | 0.4123   | 0.3264                           | 0.4441                | 0.1022   | 0.05428  | 0.1980                           | 0.01496               |
| χ <sup>2</sup>   | 0.3483   | 1.061    | 1.560                            | 3.306                 | 2.519    | 1.423    | 1.452                            | 0.8915                | 0.4928   | 0.2154   | 0.7885                           | 0.2165                |
| Langmuir isotherm  |          |          |                                  |                       |          |          |                                  |                       |          |          |                                  |                       |
| q <sub>exp</sub> , mg g <sup>-1</sup>  | 14.15    | 18.37    | 18.20                            | 17.26                 | 11.60    | 19.69    | 15.87                            | 18.35                 | 5.000    | 11.82    | 16.05                            | 9.672                 |
| q <sub>max</sub> , mg g <sup>-1</sup>  | 16.28    | 26.00    | 22.90                            | 19.94                 | 18.43    | 76.25    | 20.78                            | 27.23                 | 7.144    | 19.57    | 22.67                            | 14.31                 |
| K <sub>L</sub> , L mg <sup>-1</sup>  | 0.01533  | 0.02308  | 0.02417                          | 0.03220               | 0.004151 | 0.01469  | 0.01223                          | 0.02607               | 0.003601 | 0.004510 | 0.01066                          | 0.003846              |
| R <sub>L</sub>   | 0.06019  | 0.04106  | 0.03833                          | 0.02975               | 0.1919   | 0.06324  | 0.07323                          | 0.03712               | 0.2212   | 0.2193   | 0.08452                          | 0.2226                |
| R <sup>2</sup>   | 0.9855   | 0.9951   | 0.9875                           | 0.9871                | 0.9922   | 0.9942   | 0.9965                           | 0.9930                | 0.9965   | 0.9985   | 0.9977                           | 0.9925                |
| SSE  | 3.352    | 1.790    | 4.550                            | 4.310                 | 1.288    | 2.446    | 0.9990                           | 2.649                 | 0.1189   | 0.2470   | 0.6618                           | 0.7724                |
| RMSE   | 0.4190   | 0.2238   | 0.5687                           | 0.5388                | 0.1610   | 0.3058   | 0.1249                           | 0.3311                | 0.01486  | 0.03088  | 0.08272                          | 0.09654               |
| χ <sup>2</sup>   | 1.100    | 0.5028   | 1.148                            | 1.346                 | 1.168    | 1.052    | 0.4461                           | 1.208                 | 0.09052  | 0.7058   | 0.5435                           | 0.9263                |
| Dubinin–Radushkevich isotherm  |          |          |                                  |                       |          |          |                                  |                       |          |          |                                  |                       |
| β, mol <sup>2</sup> kJ <sup>-2</sup>   | 0.004023 | 0.004824 | 0.004413                         | 0.004113              | 0.006141 | 0.006355 | 0.004671                         | 0.004598              | 0.005420 | 0.005923 | 0.004868                         | 0.005589              |
| q <sub>D</sub> , mmol g <sup>-1</sup>  | 0.092    | 0.284    | 0.199                            | 0.160                 | 0.126    | 1.628    | 0.129                            | 0.252                 | 0.030    | 0.105    | 0.135                            | 0.064                 |
| E, kJ mol <sup>-1</sup>  | 11.15    | 10.18    | 10.64                            | 11.03                 | 9.023    | 8.870    | 10.35                            | 10.43                 | 9.605    | 9.188    | 10.13                            | 9.459                 |
| R <sup>2</sup>   | 0.9990   | 0.9971   | 0.9973                           | 0.9865                | 0.9790   | 0.9944   | 0.9975                           | 0.9944                | 0.9855   | 0.9995   | 0.9987                           | 0.9991                |
| SSE  | 0.2401   | 1.071    | 0.9677                           | 4.501                 | 3.490    | 2.345    | 0.7117                           | 2.133                 | 0.4916   | 0.08672  | 0.3855                           | 0.08916               |
| RMSE   | 0.03001  | 0.1338   | 0.1210                           | 0.5626                | 0.4362   | 0.2931   | 0.08896                          | 0.2666                | 0.06145  | 0.01084  | 0.04819                          | 0.01114               |
| χ <sup>2</sup>   | 0.6364   | 0.3554   | 0.7018                           | 2.211                 | 1.777    | 0.9670   | 0.5477                           | 0.3458                | 0.2258   | 0.2032   | 0.1627                           | 0.08253               |
| Sips isotherm  |          |          |                                  |                       |          |          |                                  |                       |          |          |                                  |                       |
| q <sub>max</sub> , mg g <sup>-1</sup>  | 20.47    | 37.67    | 43.76                            | 24.92                 | 13.66    | 47.29    | 27.25                            | 38.36                 | 6.424    | 28.75    | 30.89                            | 45.56                 |
| K <sub>S</sub> , (L mg <sup>-1</sup> ) <sup>1/n<sub>S</sub></sup>                    | 0.02165  | 0.02390  | 0.02490                          | 0.03820               | 0.001418 | 0.02050  | 0.01657                          | 0.02757               | 0.002275 | 0.004534 | 0.01353                          | 0.003849              |
| 1/n <sub>S</sub>   | 0.5597   | 0.8058   | 0.6871                           | 0.8047                | 0.654    | 1.116    | 0.8069                           | 0.8092                | 0.531    | 0.8338   | 0.8161                           | 0.6704                |
| R <sup>2</sup>   | 0.9994   | 0.9974   | 0.9967                           | 0.9911                | 0.9986   | 0.9947   | 0.9994                           | 0.9956                | 0.9973   | 0.9999   | 0.9998                           | 0.9994                |
| SSE  | 0.1413   | 0.9551   | 1.217                            | 2.975                 | 0.2299   | 2.216    | 0.1592                           | 1.649                 | 0.09230  | 0.02221  | 0.05471                          | 0.06297               |
| RMSE   | 0.01766  | 0.1194   | 0.1521                           | 0.3719                | 0.02874  | 0.2770   | 0.01990                          | 0.2061                | 0.01154  | 0.002776 | 0.006839                         | 0.007871              |
| χ <sup>2</sup>   | 0.2736   | 0.2481   | 0.7924                           | 1.531                 | 0.6384   | 0.7592   | 0.2710                           | 0.2835                | 0.2552   | 0.1195   | 0.08089                          | 0.1204                |

transmission spectroscopy instead of FTIR/PAS (photoacoustic spectroscopy).

### 3.6. Determination of the parameters in the adsorption isotherms

The parameters calculated from the Freundlich, Langmuir, D–R and Sips models, as well as the values of the coefficient of determination ( $R^2$ ) and the error functions (SSE, RMSE and  $\chi^2$ ) for the adsorption of reactive and acid dyes, with and without the addition of auxiliary substances, are shown in Tables 3 and 4, respectively. Also, based on the estimated parameters, the theoretical isotherms were plotted and are shown, with experimental data, for the examples of reactive dye RB81 and acid dye ABk1 in Figs. 12 and 13, respectively.

The values of the parameter  $1/n_F$  estimated from the Freundlich isotherm for all dyes, with and without the addition of auxiliaries, were lower than 1, indicating the favorable nature of the adsorption. Higher values of  $K_F$  in the presence of salts and acetic acid for the adsorption of reactive dyes, and of acetic acid at pH 3.0 for the adsorption of acid dyes indicate an increase in the intensity of the adsorption of the dyes in the presence of auxiliaries. At the same time, as the pH of acetic acid increases, the adsorption intensity of acid dyes decreases (Table 4).

The Langmuir model provides useful information, such as the maximum adsorption capacity ( $q_{max}$ ) and the isotherm constant ( $K_L$ ), which is related to the affinity of the binding sites and the binding energy. The values of the parameter  $q_{max}$  for all dye-auxiliary substance systems were greater than

Table 4  
Isotherm parameters, the values of coefficient of determination and error functions for the adsorption of acid dyes

|  | ABk1     | +CH <sub>3</sub> COOH<br>pH = 3.0 | +CH <sub>3</sub> COOH<br>pH = 4.6 | AB9      | +CH <sub>3</sub> COOH<br>pH = 3.0 | +CH <sub>3</sub> COOH<br>pH = 4.6 |
|--|----------|-----------------------------------|-----------------------------------|----------|-----------------------------------|-----------------------------------|
| Freundlich isotherm                                |          |                                   |                                   |          |                                   |                                   |
| $1/n_F$  | 0.4645   | 0.5198                            | 0.3998                            | 0.6454   | 0.5712                            | 0.5184                            |
| $K_F, \text{mg g}^{-1} (\text{L mg}^{-1})^{1/n_F}$ | 2.185    | 4.064                             | 2.115                             | 0.1087   | 0.2339                            | 0.1252                            |
| $R^2$  | 0.9911   | 0.9945                            | 0.9301                            | 0.9702   | 0.9905                            | 0.9848                            |
| SSE  | 3.167    | 2.19                              | 22.43                             | 1.768    | 0.8049                            | 0.2757                            |
| RMSE   | 0.3959   | 0.2744                            | 2.803                             | 0.2210   | 0.1006                            | 0.03446                           |
| $\chi^2$   | 1.799    | 1.652                             | 6.270                             | 0.6992   | 0.5067                            | 0.3333                            |
| Langmuir isotherm                                  |          |                                   |                                   |          |                                   |                                   |
| $q_{exp}, \text{mg g}^{-1}$                        | 17.67    | 19.65                             | 16.50                             | 6.670    | 8.300                             | 3.778                             |
| $q_{max}, \text{mg g}^{-1}$                        | 19.60    | 25.28                             | 17.64                             | 11.32    | 11.65                             | 4.927                             |
| $K_L, \text{L mg}^{-1}$                            | 0.05904  | 0.1406                            | 0.05576                           | 0.002380 | 0.004310                          | 0.004067                          |
| $R_L$  | 0.01702  | 0.007030                          | 0.01698                           | 0.2933   | 0.1914                            | 0.1967                            |
| $R^2$  | 0.9843   | 0.9855                            | 0.9939                            | 0.9909   | 0.9980                            | 0.9969                            |
| SSE  | 5.557    | 5.824                             | 1.957                             | 0.5410   | 0.1665                            | 0.05590                           |
| RMSE   | 0.6946   | 0.7280                            | 0.2446                            | 0.06762  | 0.02081                           | 0.006988                          |
| $\chi^2$   | 2.089    | 5.166                             | 1.449                             | 0.3017   | 0.1897                            | 0.06487                           |
| Dubinin–Radushkevich isotherm                      |          |                                   |                                   |          |                                   |                                   |
| $\beta, \text{mol}^2 \text{kJ}^{-2}$               | 0.003591 | 0.003599                          | 0.003283                          | 0.006530 | 0.005496                          | 0.005173                          |
| $q_D, \text{mmol g}^{-1}$                          | 0.154    | 0.317                             | 0.102                             | 0.066    | 0.063                             | 0.022                             |
| $E, \text{kJ mol}^{-1}$                            | 11.80    | 11.79                             | 12.34                             | 8.751    | 9.538                             | 9.831                             |
| $R^2$  | 0.9963   | 0.9975                            | 0.9564                            | 0.9800   | 0.9963                            | 0.9932                            |
| SSE  | 1.322    | 1.021                             | 13.98                             | 1.191    | 0.3133                            | 0.1232                            |
| RMSE   | 0.1653   | 0.1277                            | 1.748                             | 0.1489   | 0.03916                           | 0.01540                           |
| $\chi^2$   | 0.7995   | 1.032                             | 4.401                             | 0.4930   | 0.1666                            | 0.1213                            |
| Sips isotherm                                      |          |                                   |                                   |          |                                   |                                   |
| $q_{max}, \text{mg g}^{-1}$                        | 33.62    | 53.63                             | 17.42                             | 8.011    | 13.62                             | 5.561                             |
| $K_{s,r} (\text{L mg}^{-1})^{1/n_s}$               | 0.0586   | 0.0998                            | 0.0532                            | 0.00435  | 0.00580                           | 0.0958                            |
| $1/n_s$  | 0.6402   | 0.6441                            | 1.031                             | 0.450    | 0.8852                            | 0.8862                            |
| $R^2$  | 0.9963   | 0.9972                            | 0.9940                            | 0.9973   | 0.9988                            | 0.9977                            |
| SSE  | 1.322    | 1.139                             | 1.934                             | 0.1577   | 0.1030                            | 0.04090                           |
| RMSE   | 0.1652   | 0.1424                            | 0.2417                            | 0.01971  | 0.01288                           | 0.005113                          |
| $\chi^2$   | 0.7214   | 1.118                             | 1.485                             | 3.711    | 0.07084                           | 0.03137                           |

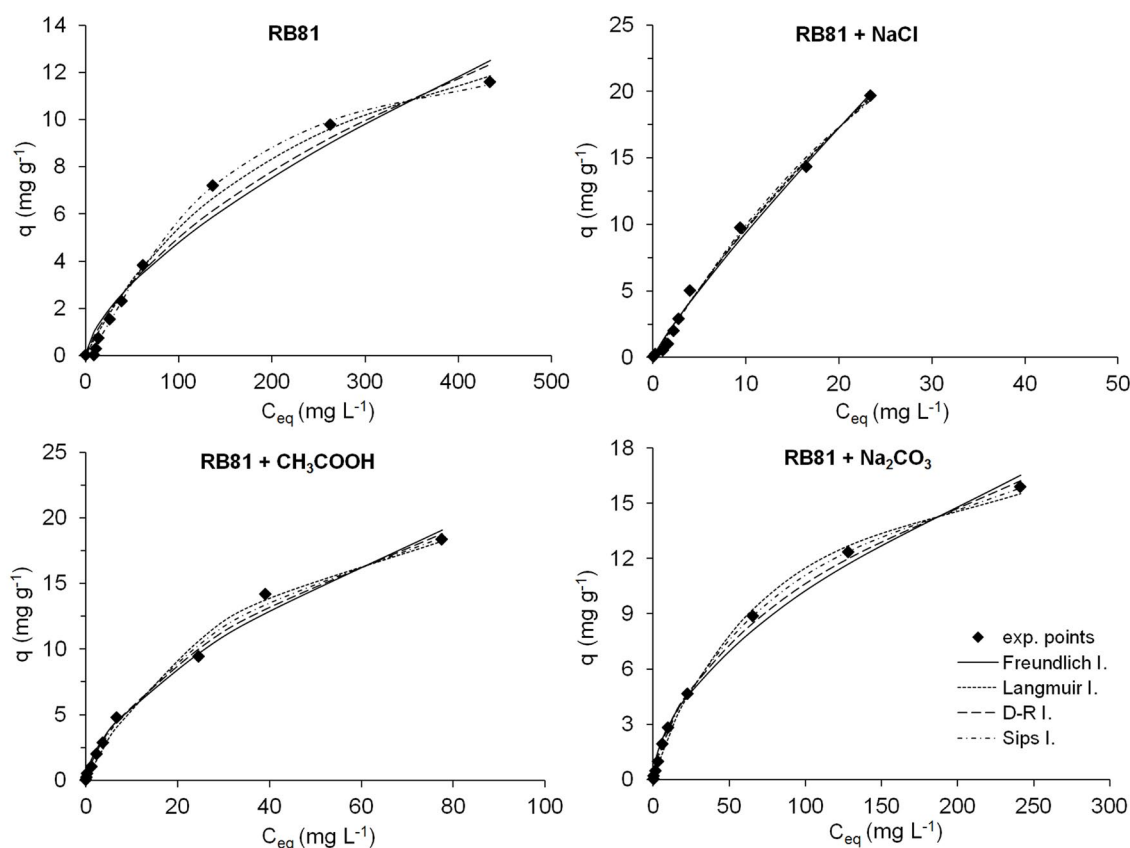
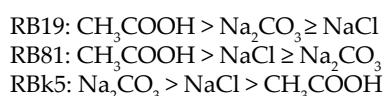


Fig. 12. Reactive Blue 81 adsorption isotherms on low-moor peat; the lines are the plots of theoretical isotherm models.

the experimental values, which indicates that the monolayer was not completely covered. An increase in the values of  $K_L$  in the presence of auxiliaries indicates an increase in the affinity of the dye for the peat. The effect of auxiliaries on the affinity of reactive dyes for the peat surface depended on the dye-auxiliary substance system and changed in the following order:



Acid dyes in the presence of  $\text{CH}_3\text{COOH}$  at pH 3.0 also showed a higher affinity to the peat surface, whereas in the presence of  $\text{CH}_3\text{COOH}$  at pH 4.6, the affinity of the dyes to the surface was at the same level as that of the dyes without auxiliaries. The values of  $R_L$  calculated from Eq. (7) indicated that the adsorption process was favorable for all systems.

The values of  $E$  estimated from the D–R model were found to be higher than  $8 \text{ kJ mol}^{-1}$ , which indicates that the process was a chemical adsorption.

The values of  $1/n_s$  calculated from the Sips model indicated that the addition of auxiliary substances to the solution increased the heterogeneity of all systems, and the  $1/n_s$  values were at the  $1/n_f$  level for reactive dyes and higher for acid dyes. The values of the parameter  $K_s$  at the  $K_L$  level estimated from the Langmuir isotherm indicated a positive effect of auxiliaries on the adsorption process.

The values of coefficient of determination  $R^2$ , in the range of 0.9662–0.9999 for the adsorption of reactive dyes and in the range of 0.9301–0.9988 for acid dyes, indicate that the experimental isotherm data of the tested dyes can be described with all four adsorption models. However, the lowest values of the error function SSE, RMSE and  $\chi^2$  showed that the Sips isotherm is the best-fit model for the adsorption process (Figs. 12 and 13). The model combines elements from both the Langmuir and Freundlich equations, suggesting that the mechanism of dye binding is more complex and does not follow an ideal monolayer adsorption. Similar results were obtained by other authors investigating the adsorption of dyes on organic adsorbents [37,56].

Furthermore, the studies on the removal of cationic dyes with the use of peat carried out by Chieng et al. [58] indicate that the three-parameter models provide a better fit to the experimental data than do the two-parameter models.

#### 4. Conclusions

The results show that the presence of auxiliary substances  $\text{NaCl}$ ,  $\text{Na}_2\text{CO}_3$  and  $\text{CH}_3\text{COOH}$  used in real dyeing processes had a strong effect on the adsorption capacity of low-moor peat for reactive dyes Reactive Blue 19, Reactive Blue 81, and Reactive Black 5 and acid dyes Acid Black 1 and Acid Blue 9. The effect of auxiliary substances depended on the dye-adsorbent system: the lower the binding ability of the dye to the peat, the greater the effect of the auxiliary substances.

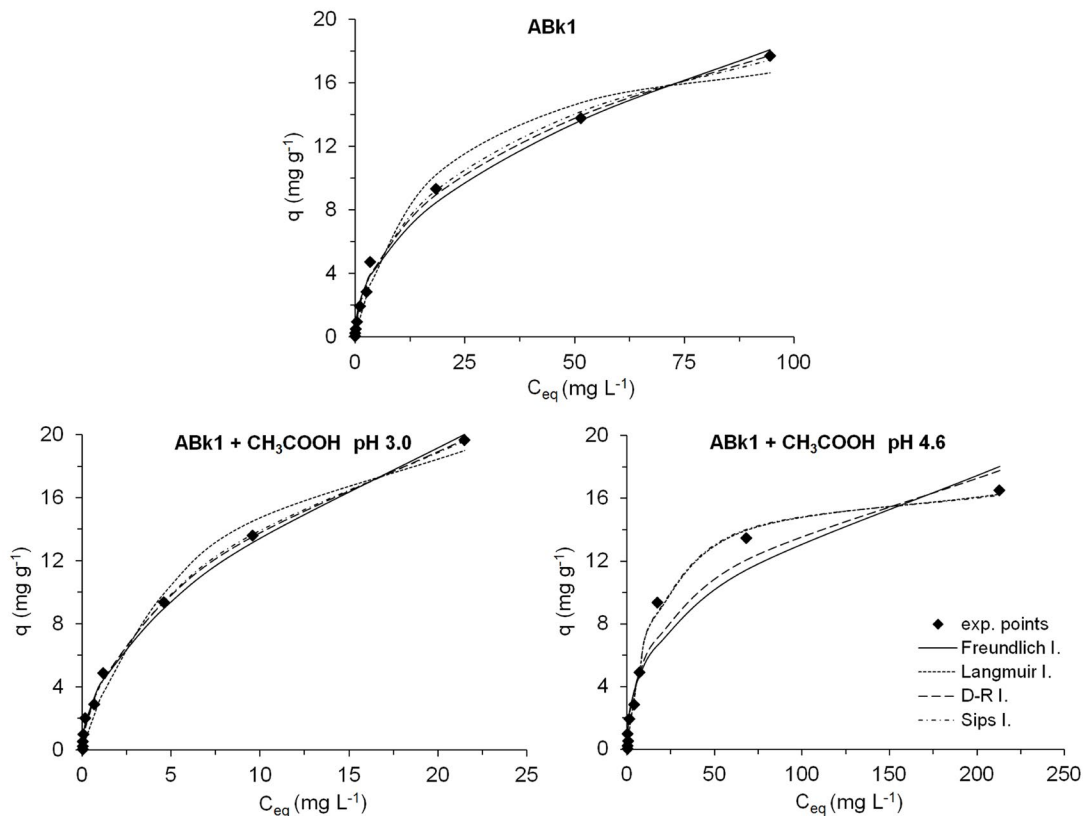


Fig. 13. Theoretical isotherms with experimental points of Acid Black 1 adsorption with the addition of  $\text{CH}_3\text{COOH}$ .

According to the estimated values of the parameters in the Langmuir, Freundlich, D–R, and Sips isotherm models, the maximum dyes adsorption capacity, the affinity of the binding sites and the binding energy, as well as the intensity of adsorption, increased in the presence of the auxiliary substances in the solution.

The presence of  $\text{CH}_3\text{COOH}$  was an important factor since the  $\text{H}^+$  in the solution affected the peat surface charge by protonation and a possibility of binding anionic dyes via electrostatic interaction. Only  $\text{CH}_3\text{COOH}$  at low pH affected the peat surface charge because of the very good buffering capacity of peat.  $\text{NaCl}$  and  $\text{Na}_2\text{CO}_3$  increased the intermolecular forces, as well as the dimerization process, of reactive dyes in the solution.

The Sips equation fits the experimental results best. The model combines elements from both the Langmuir and Freundlich equations, suggesting that the mechanism of dye binding is more complex and does not follow an ideal monolayer adsorption.

The results also indicate that when testing new substances to be used as adsorbents for the removal of dyes from water and wastewater their actual composition should be taken into account, including the presence of auxiliary substances, which have a significant impact on the adsorption process.

#### Acknowledgments

This study was supported by the Polish Ministry of Science and Higher Education Project No. N523 3509 33

and by National Science Centre project No 2012/05/N/ST8/03149.

#### Symbols

|                  |   |  |
|------------------|---|--|
| $q$              | — | Amount of dye adsorbed per unit mass of the adsorbent, $\text{mg g}^{-1}$ or $\text{mmol g}^{-1}$  |
| RE               | — | Removal efficiency, %  |
| $C_0$            | — | Initial dye concentration, $\text{mg L}^{-1}$  |
| $C_{\text{eq}}$  | — | Equilibrium dye concentration, $\text{mg L}^{-1}$  |
| $V$              | — | Volume of the solution, $\text{cm}^3$  |
| $m$              | — | Mass of the adsorbent, g   |
| $K_F$            | — | Freundlich equilibrium constant related to the adsorption capacity and adsorption intensity of the system, $\text{mg g}^{-1} (\text{L mg}^{-1})^{1/n_F}$ |
| $1/n_F$          | — | Expresses favorability of adsorption, dimensionless  |
| $q_{\text{max}}$ | — | Maximum adsorption capacity, $\text{mg g}^{-1}$  |
| $K_L$            | — | Langmuir constant related to the affinity of the binding sites and the energy of adsorption, $\text{L mg}^{-1}$  |
| $R_L$            | — | Separation factor, dimensionless   |
| $q_D$            | — | Theoretical saturation capacity, $\text{mmol g}^{-1}$  |
| $\beta$          | — | Constant related to the adsorption energy, $\text{mol}^2 \text{kJ}^{-2}$   |
| $\varepsilon$    | — | Polanyi potential  |
| $R$              | — | Gas constant, $\text{J mol}^{-1} \text{K}^{-1}$  |
| $T$              | — | Temperature, K   |
| $E$              | — | Mean free energy of adsorption per molecule of the adsorbate, $\text{kJ mol}^{-1}$   |

|           |   |   |
|-----------|---|---|
| $K_S$     | — | Sips constant related with affinity constant, $(L\ mg^{-1})^{1/n^S}$    |
| $1/n_S$   | — | Sips exponent which represents the surface heterogeneity, dimensionless |
| $R^2$     | — | Coefficient of determination  |
| $\chi^2$  | — | Nonlinear chi-square test   |
| $q_{cal}$ | — | Calculated value of adsorption capacity, $mg\ g^{-1}$                   |
| $q_{exp}$ | — | Experimental value of adsorption capacity, $mg\ g^{-1}$                 |
| $n$       | — | Number of observations in the experimental data                         |

## References

- [1] L.A. Sepulveda, C.C. Santana, Effect of solution temperature, pH and ionic strength on dye adsorption onto Magellanic peat, *Environ. Technol.*, 34 (2013) 967–977.
- [2] C. Zaharia, D. Suteu, Textile Organic Dyes – Characteristics, Polluting Effects and Separation/Elimination Procedures from Industrial Effluents – A Critical Overview, Chapter 3, T. Puzyn, Ed., Organic Pollutants Ten Years After the Stockholm Convention - Environmental and Analytical Update, InTech-Open, Rijeka, Croatia, 2012, pp. 55–86.
- [3] L. Sepulveda, F. Troncoso, E. Contreras, C. Palma, Competitive adsorption of textile dyes using peat: adsorption equilibrium and kinetic studies in monosolute and bisolute systems, *Environ. Technol.*, 29 (2008) 947–957.
- [4] S. Venkata Mohan, P. Sailaja, M. Srimurali, J. Karthikeyan, Color removal of monoazo acid dye from aqueous solution by adsorption and chemical coagulation, *Environ. Eng. Policy*, 1 (1999) 149–154.
- [5] E.A. Clarke, R. Anliker, In: O. Hutzinger, Ed., The Handbook of Environmental Chemistry, Vol. 3A, Springer-Verlag, Berlin, 1980, pp. 181–215.
- [6] T. Józwiak, U. Filipkowska, J. Rodziewicz, A. Mielcarek, D. Owczarkowska, Application of compost as a cheap sorbent for dyes removal from aqueous solutions, *Rocz. Ochr. Sr.*, 15 (2013) 2398–2411, (In Polish).
- [7] A.N. Fernandes, C.A.P. Almeida, C.T.B. Menezes, N.A. Debacher, M.M.D. Sierra, Removal of methylene blue from aqueous solution by peat, *J. Hazard. Mater.*, 144 (2007) 412–419.
- [8] I.M. Banat, P. Nigam, D. Singh, R. Marchant, Microbial decolorization of textile-dye-containing effluents: a review, *Bioresour. Technol.*, 58 (1996) 217–227.
- [9] T. Robinson, G. McMullan, R. Marchant, P. Nigam, Remediation of dyes in textile effluent: a critical review on current treatment technologies with a proposed alternative, *Bioresour. Technol.*, 77 (2001) 247–255.
- [10] L. Bilińska, S. Ledakowicz, Possibilities of using advanced oxidation processes - AOP for the textile wastewater treatment in industrial conditions, *Informator Chemika Kolorysty*, 17 (2011) 21–35, (In Polish).
- [11] S.M. Burkinshaw, G. Salihu, The role of auxiliaries in the immersion dyeing of textile fibres: part 1 an overview, *Dyes Pigm.*, 161 (2019) 519–530.
- [12] S.M. Burkinshaw, G. Salihu, The role of auxiliaries in the immersion dyeing of textile fibres: part 7 theoretical models to describe the mechanism by which inorganic electrolytes promote reactive dye uptake on cellulosic fibres, *Dyes Pigm.*, 161 (2019) 605–613.
- [13] A. Khatri, M. White, R. Padhye, Effect of dye solution ionic strength on dyeing of cotton with reactive dyes, *Fiber Polym.*, 19 (2018) 1266–1270.
- [14] A.W.M. Ip, J.P. Barford, G. McKay, Reactive black dye adsorption/desorption onto different adsorbents: effect of salt, surface chemistry, pore size and surface area, *J. Colloid Interface Sci.*, 337 (2009) 32–38.
- [15] J. Kyzioł-Komosińska, Cz. Rosik-Dulewska, A. Dzieniszewska, M. Pająk, Low-moor peats as biosorbents for removal of anionic dyes from water, *Fresenius Environ. Bull.*, 27 (2018) 6–20.
- [16] L.A. Sepulveda-Cuevas, E.G. Contreras-Villacura, C.L. Palma-Tolosa, Magellan peat (*Sphagnum magallanicum*) as natural adsorbent of recalcitrant synthetic dyes, *J. Soil Sci. Plant Nutr.*, 8 (2008) 31–43.
- [17] S. Rovani, A.N. Fernandes, L.D.T. Prola, E.C. Lima, W.O. Santos, M.A. Adebayo, Removal of Cibacron Brilliant Yellow 3G-P dye from aqueous solutions by Brazilian peats as biosorbents, *Chem. Eng. Commun.*, 201 (2014) 1431–1458.
- [18] J. Kyzioł-Komosińska, Cz. Rosik-Dulewska, M. Pająk, J. Czupioł, A. Dzieniszewska, I. Krzyżewska, Sorption of Acid Green 16 from aqueous solution onto low-moor peat and smectite clay co-occurring in lignite of Belchatow mine field, *Rocz. Ochr. Sr.*, 17 (2015) 165–187.
- [19] P. Janos, P. Michalek, L. Turek, Sorption of ionic dyes onto untreated low-rank coal - oxihumolite: a kinetic study, *Dyes Pigm.*, 74 (2007) 363–370.
- [20] A. Hassani, F. Vafaei, S. Karaca, A.R. Khataee, Adsorption of a cationic dye from aqueous solution using Turkish lignite: kinetic, isotherm, thermodynamic studies and neural network modeling, *J. Ind. Eng. Chem.*, 20 (2014) 2615–2624.
- [21] G. McKay, J.F. Porter, G.R. Prasad, The removal of dye colours from aqueous solutions by adsorption on low-cost materials, *Water Air Soil Pollut.*, 114 (1999) 423–438.
- [22] M.S. Tanyildizi, Modeling of adsorption isotherms and kinetics of reactive dye from aqueous solution by peanut hull, *Chem. Eng. J.*, 168 (2011) 1234–1240.
- [23] M. Asgher, H.N. Bhatti, Evaluation of thermodynamics and effect of chemical treatments on sorption potential of *Citrus waste* biomass for removal of anionic dyes from aqueous solutions, *Ecol. Eng.*, 38 (2012) 79–85.
- [24] G.E. do Nascimento, N.F. Campos, J.J. da Silva, C.M.B. de Menezes Barbosa, M.M.M.B. Duarte, Adsorption of anionic dyes from an aqueous solution by banana peel and green coconut mesocarp, *Desal. Wat. Treat.*, 57 (2016) 14093–14108.
- [25] K. Vasanth Kumar, S. Sivanesan, Sorption isotherm for safranin onto rice husk: comparison of linear and non-linear methods, *Dyes Pigm.*, 72 (2007) 130–133.
- [26] S. Parvin, W. Rahman, I. Saha, J. Alam, M.R. Khan, Coconut tree bark as a potential low-cost adsorbent for the removal of methylene blue from wastewater, *Desal. Wat. Treat.*, 146 (2019) 385–392.
- [27] N.M. Mahmoodi, B. Hayati, M. Arami, C. Lan, Adsorption of textile dyes on *Pine Cone* from colored wastewater: kinetic, equilibrium and thermodynamic studies, *Desalination*, 268 (2011) 117–125.
- [28] M. Kaya, Evaluation of a novel woody waste obtained from tea tree sawdust as an adsorbent for dye removal, *Wood Sci. Technol.*, 52 (2018) 245–260.
- [29] M. Fabbicino, B. Naviglio, G. Tortora, L. d’Antonio, An environmental friendly cycle for Cr(III) removal and recovery from tannery wastewater, *J. Environ. Manage.*, 117 (2013) 1–6.
- [30] J. Kanagaraj, T. Senthilvelan, R.C. Panda, R. Aravindhan, A.B. Mandal, Biosorption of trivalent chromium from wastewater: an approach towards green chemistry, *Chem. Eng. Technol.*, 37 (2014) 1741–1750.
- [31] J. Kyzioł-Komosińska, I. Twardowska, J. Kocela, Adsorption of cadmium(II) ions from industrial wastewater by low moor peat occurring in the overburden of brown coal deposits, *Arch. Environ. Prot.*, 34 (2008) 83–95.
- [32] S.J. Allen, G. McKay, J.F. Porter, Adsorption isotherm models for basic dye adsorption by peat in single and binary component systems, *J. Colloid Interface Sci.*, 280 (2004) 322–333.
- [33] L. Rusu, M. Harja, A.I. Simion, D. Suteu, G. Ciobanu, L. Favier, Removal of Atrazine Blue from aqueous solutions onto brown peat. equilibrium and kinetics studies, *Korean J. Chem. Eng.*, 31 (2014) 1008–1015.
- [34] Website of the Producer of Peat Products, Available at: [www.torf.net.pl](http://www.torf.net.pl).
- [35] Website of the Producer of Activated Carbon, Available at: [www.desotec.com/pl](http://www.desotec.com/pl).
- [36] D. Pathania, A. Sharma, Z.-M. Siddiqi, Removal of congo red dye from aqueous system using *Phoenix dactylifera* seeds, *J. Mol. Liq.*, 219 (2016) 359–367.
- [37] H.I. Chieng, L.B.L. Lim, N. Priyantha, D.T.B. Tennakoon, Sorption characteristics of peat of Brunei Darussalam III:

- equilibrium and kinetics studies on adsorption of Crystal Violet (CV), *Int. J. Earth Sci. Eng.*, 6 (2013) 791–801.
- [38] J. Kyzioł-Komosińska, F. Barba, P. Callejas, C. Rosik-Dulewska, Beidellite and other natural low-cost sorbents to remove chromium and cadmium from water and wastewater, *Bol. Soc. Esp. Ceram. Vidrio*, 49 (2010) 121–128.
- [39] G. Rangel-Porras, J.B. Garcia-Magno, M.P. Gonzalez-Munoz, Lead and cadmium immobilization on calcitic limestone materials, *Desalination*, 262 (2010) 1–10.
- [40] C.H. Giles, D. Smith, A. Huitson, A general treatment and classification of the solute adsorption isotherm. I. Theoretical, *J. Colloid Interface Sci.*, 47 (1974) 755–765.
- [41] J.C.P. Vagheti, E.C. Lima, B. Royer, B.M. da Cunha, N.F. Cardoso, J.L. Brasil, S.L.P. Dias, Pecan nutshell as biosorbent to remove Cu(II), Mn(II) and Pb(II) from aqueous solutions, *J. Hazard. Mater.*, 162 (2009) 270–280.
- [42] H.M.F. Freundlich, Over the adsorption in solution, *J. Phys. Chem.*, 57 (1906) 385–471.
- [43] K.Y. Foo, B.H. Hameed, Insights into the modeling of adsorption isotherm systems, *Chem. Eng. J.*, 156 (2010) 2–10.
- [44] P.A. Brown, S.A. Gill, S.J. Allen, Metal removal from wastewater using peat, *Water Res.*, 34 (2000) 3907–3916.
- [45] I. Langmuir, The constitution and fundamental properties of solids and liquids. Part I. Solids, *J. Am. Chem. Soc.*, 38 (1916) 2221–2295.
- [46] A. Celekli, G. Ilgun, H. Bozkurt, Sorption equilibrium, kinetic, thermodynamic, and desorption studies of reactive red 120 on *Chara contraria*, *Chem. Eng. J.*, 191 (2012) 228–235.
- [47] M.M. Dubinin, The potential theory of adsorption of gases and vapors for adsorbents with energetically nonuniform surfaces, *Chem. Rev.*, 60 (1960) 235–241.
- [48] R. Sips, On the structure of a catalyst surface, *J. Chem. Phys.*, 16 (1948) 490–495.
- [49] G. McKay, M. Hadi, M.T. Samadi, A.R. Rahmani, M.S. Aminabad, F. Nazemi, Adsorption of reactive dye from aqueous solutions by compost, *Desal. Wat. Treat.*, 28 (2011) 164–173.
- [50] M. Cybulak, Z. Sokołowska, P. Boguta, A. Tomczyk, Influence of pH and grain size on physicochemical properties of biochar and released humic substances, *Fuel*, 240 (2019) 334–338.
- [51] H. Gonzalez-Raymat, V. Anagnostopoulos, M. Denham, V. Cai, Y.P. Katsenovich, Unrefined humic substances as a potential low-cost amendment for the management of acidic groundwater contamination, *J. Environ. Manage.*, 212 (2018) 210–218.
- [52] X. Li, T. Liu, F. Li, W. Zhang, S. Zhou, Y. Li, Reduction of structural Fe(III) in oxyhydroxides by *Shewanella decolorationis* S12 and characterization of the surface properties of iron minerals, *J. Soil. Sediment.*, 12 (2012) 217–227.
- [53] J. Kyzioł-Komosińska, L. Kukułka, Application of Minerals Co-occurring in Brown Coal Deposits to Removal of Heavy Metals from Water and Wastewater, Works and Studies 75, Institute of Environmental Engineering of the Polish Academy of Sciences, Zabrze, 2008, (In Polish).
- [54] G.Z. Kyzas, N.K. Lazaridis, A.Ch. Mitropoulos, Removal of dyes from aqueous solutions with untreated coffee residues as potential low-cost adsorbents: equilibrium, reuse and thermodynamic approach, *Chem. Eng. J.*, 189–190 (2012) 148–159.
- [55] Y.S. Al-Degs, M.I. El-Barghouthi, A.H. El-Sheikh, G.M. Walker, Effect of solution pH, ionic strength, and temperature on adsorption behavior of reactive dyes on activated carbon, *Dyes Pigm.*, 77 (2008) 16–23.
- [56] K. Vijayaraghavan, Y. Premkumar, J. Jegan, Malachite green and crystal violet biosorption onto coco-peat: characterization and removal studies, *Desal. Wat. Treat.*, 57 (2016) 6423–6431.
- [57] P. Janos, P. Sedivy, M. Ryznarova, S. Grotchelova, Sorption of basic and acid dyes from aqueous solutions onto oxihumolite, *Chemosphere*, 59 (2005) 881–886.
- [58] H.I. Chieng, T. Zehra, L.B.L. Lim, N. Priyantha, D.T.B. Tennakoon, Sorption characteristics of peat of Brunei Darussalam IV: equilibrium, thermodynamics and kinetics of adsorption of methylene blue and malachite green dyes from aqueous solution, *Environ. Earth Sci.*, 72 (2014) 2263–2277.